IOP Publishing Measurement Science and Technology
Meas. Sci. Technol. **28** (2017) 115004 (8pp) https://doi.org/10.1088/1361-6501/aa8373

JY1 time scale: a new Kalman-filter time scale designed at NIST

Jian Yao[1,2], Thomas E Parker[1] and Judah Levine[1,2]

[1] Time and Frequency Division, National Institute of Standards and Technology, Boulder, CO, United States of America
[2] Department of Physics, University of Colorado at Boulder, Boulder, CO, United States of America

E-mail: jian.yao@nist.gov

Received 13 March 2017, revised 28 July 2017
Accepted for publication 2 August 2017
Published 17 October 2017

Abstract

We report on a new Kalman-filter hydrogen-maser time scale (i.e. JY1 time scale) designed at the National Institute of Standards and Technology (NIST). The JY1 time scale is composed of a few hydrogen masers and a commercial Cs clock. The Cs clock is used as a reference clock to ease operations with existing data. Unlike other time scales, the JY1 time scale uses three basic time-scale equations, instead of only one equation. Also, this time scale can detect a clock error (i.e. time error, frequency error, or frequency drift error) automatically. These features make the JY1 time scale stiff and less likely to be affected by an abnormal clock. Tests show that the JY1 time scale deviates from the UTC by less than ±5 ns for ~100 d, when the time scale is initially aligned to the UTC and then is completely free running. Once the time scale is steered to a Cs fountain, it can maintain the time with little error even if the Cs fountain stops working for tens of days. This can be helpful when we do not have a continuously operated fountain or when the continuously operated fountain accidentally stops, or when optical clocks run occasionally.

Keywords: time scale, Kalman filter, atomic clock, hydrogen maser, cesium fountain clock, UTC

(Some figures may appear in colour only in the online journal)

1. Introduction

At timing laboratories, we require a time scale to be accurate, precise, and reliable [1]. By definition, a Cs fountain is naturally accurate. However, a Cs fountain is typically noisier than a hydrogen maser (H-maser) for an averaging time of less than several days. Thus, those labs that run a Cs fountain continuously, such as the Observatoire de Paris in France and Physikalisch-Technische Bundesanstalt in Germany, have formed a time scale composed of a Cs fountain and an H-maser [2, 3]. The short-term output of the time scale is determined by the H-maser, while the long-term output of the time scale is determined by the Cs fountain. In this way, the time scale is both accurate and precise. To improve reliability, an additional back-up H-maser is added in the time scale [2, 3], to avoid the consequence of an H-maser failure.

In this paper, we propose a different architecture for a time scale. The time scale is composed of an occasionally operated Cs fountain and a clock ensemble. The clock ensemble is composed of several H-maser clocks and a commercial Cs clock. The commercial Cs clock is chosen as a reference clock for its reliability and for easy operation with existing data. The clock ensemble, forming a free-running time scale using a Kalman filter, is steered to the Cs fountain. Since we have several H-masers, the short-term stability of the time scale is better than a single H-maser due to averaging. Also, it is easier to detect and mitigate unobvious clock errors (such as a small frequency step, or a small frequency-drift step), which improves the reliability of the time scale. Besides, unlike Greenhall's time scale [4–6] and Galleani and Tavella's time scale [7, 8], the new Kalman-filter time scale presented in this paper uses three basic time-scale equations instead of only one equation. This characteristic gives the time scale a better long-term stability, which allows the Cs fountain to stop working for tens of days without significant degradation.

In section 2, we will discuss the basic principle of the time scale. Section 3 will test the performance of the free-running time scale. In section 4, we will steer the free-running time scale to a Cs fountain and form the final time scale. Note, all the data used in this paper are real measurement data, except where mentioned specifically.

2. Kalman-filter H-maser time scale

The Kalman filter has been widely used to make predictions based on real-time measurements. The fundamental assumption in a Kalman filter is that the noise type in both the measurement and physical quantity is white. Although the clock behavior is only approximately white, the Kalman filter still works well [4–10].

In the Kalman filter, there are two basic equations, i.e. equations (1) and (2). Equation (1) is called the system model, which describes what the predicted state of the system will be at epoch $k+1$, based on its state at epoch k. Here, $X(k)$ is the estimated state vector of the system at epoch k, and $X(k+1|k)$ is the predicted state vector of the system at epoch $k+1$. Φ is called the transition matrix, which links $X(k)$ and $X(k+1|k)$. Φ is determined by the physical property of the system. u is the process noise, which is characterized by the Q matrix. Equation (2) is called the measurement model. The H matrix, called the observation matrix, gives the relation between the state vector X and the measurement vector Z. v is the measurement noise, which is characterized by the R matrix

$$X(k+1|k) = \Phi \cdot X(k) + u, \quad u \sim N(0, Q), \tag{1}$$

$$Z(k+1) = H \cdot X(k+1|k) + v, \quad v \sim N(0, R). \tag{2}$$

Based on the principle of a Kalman filter, the estimated state vector of the system at epoch $k+1$ should be

$$X(k+1) = X(k+1|k) + K \cdot (Z(k+1) - H \cdot X(k+1|k)), \tag{3}$$

where K is called the Kalman gain matrix. An intuitive understanding of equation (3) gives that the estimated state vector is equal to the predicted state vector plus the correction from the measurement. The Kalman gain matrix K reveals the ratio of the measurement to the prediction. The formula for calculating K is as follows:

$$K = P(k+1|k) \cdot H^T \cdot [H \cdot P(k+1|k) \cdot H^T + R], \tag{4}$$

where $P(k+1|k) = \Phi \cdot P(k) \cdot \Phi^T + Q$, and $P(k+1) = [I - K \cdot H] \cdot P(k+1|k)$.

Thus, K depends on the process noise matrix Q, the measurement noise matrix R, the initial error covariance matrix $P(0)$, the transition matrix Φ, and the observation matrix H. The derivation of equations (3) and (4) can be found in chapter 4 of [11] and is beyond the scope of this paper.

Next, we build a new Kalman-filter time scale (i.e. JY1 time scale), following the above discussion. The JY1 time scale is composed of M clocks, where one clock is a commercial Cs clock and the rest $M-1$ clocks are H-masers. The Cs clock is chosen as a reference clock to ease operations with existing data. Each clock is characterized in terms of three parameters—time, fractional frequency, and fractional frequency drift, with respect to the JY1 time scale. We model the evolution of these parameters from epoch k to epoch $k+1$ for clock i [12], by

$$x_i(k+1|k) = x_i(k) + f_i(k)\Delta t + \frac{1}{2} d_i(k)(\Delta t)^2 + \xi_i, \tag{5.1}$$

$$f_i(k+1|k) = f_i(k) + d_i(k)\Delta t + \eta_i, \tag{5.2}$$

$$d_i(k+1|k) = d_i(k) + \zeta_i, \tag{5.3}$$

where x is time, f is fractional frequency, and d is fractional frequency drift. $x_i(k)$ is the time estimate of clock i with respect to the JY1 time scale at epoch k, and $x_i(k+1|k)$ is the predicted time of clock i with respect to the JY1 time scale at epoch $k+1$. Δt stands for the time interval between epoch k and epoch $k+1$, and is 12 min for the JY1 time scale. ξ, η, ζ are the noise terms in time, fractional frequency, and fractional frequency drift. According to [5, 7, 12], ξ and η represent the white frequency noise and the random-walk frequency noise, respectively, which can be determined by the Allan variance of the clock. ζ represents the random-run frequency noise, which is typically very tiny, or even not observed, for an H-maser. Thus, we set the variance of ζ to a small value (e.g. 3.3×10^{-8} (ns d^{-2})^2) for all H-masers.

Because we have M clocks in the time scale, we generalize equations (5) and (6). Note, the left side of equation (6) is actually $X(k+1|k)$ in equation (1), and the matrix on the right side of the equal sign is actually the transition matrix Φ.

$$\begin{pmatrix} x_1(k+1|k) \\ f_1(k+1|k) \\ d_1(k+1|k) \\ \vdots \\ x_i(k+1|k) \\ f_i(k+1|k) \\ d_i(k+1|k) \\ \vdots \end{pmatrix} = \begin{pmatrix} 1 & \Delta t & \frac{1}{2}(\Delta t)^2 & & & & & & \\ 0 & 1 & \Delta t & & & O & & & \\ 0 & 0 & 1 & & & & & & \\ & & & \ddots & & & & & \\ & & & & 1 & \Delta t & \frac{1}{2}(\Delta t)^2 & & \\ & & & & 0 & 1 & \Delta t & & \\ & O & & & 0 & 0 & 1 & & \\ & & & & & & & \ddots & \end{pmatrix} \cdot \begin{pmatrix} x_1(k) \\ f_1(k) \\ d_1(k) \\ \vdots \\ x_i(k) \\ f_i(k) \\ d_i(k) \\ \vdots \end{pmatrix} + \begin{pmatrix} \xi_1 \\ \eta_1 \\ \zeta_1 \\ \vdots \\ \xi_i \\ \eta_i \\ \zeta_i \\ \vdots \end{pmatrix}, \text{where} \begin{pmatrix} \xi_1 \\ \eta_1 \\ \zeta_1 \\ \vdots \\ \xi_i \\ \eta_i \\ \zeta_i \\ \vdots \end{pmatrix} \sim N(0, Q). \tag{6}$$

Since our measurement vector $Z(k+1)$, a $(M-1) \times 1$ vector is the measured time differences between each H-maser and the reference clock at epoch $k+1$, the H matrix (note, the H matrix is a $(M-1) \times 3M$ matrix) should be as follows:

$$H = \left(\begin{array}{ccc|ccc|ccc|c|ccc} 1 & 0 & 0 & -1 & 0 & 0 & 0 & 0 & 0 & \cdots & 0 & 0 & 0 \\ 1 & 0 & 0 & 0 & 0 & 0 & -1 & 0 & 0 & \cdots & 0 & 0 & 0 \\ \vdots & \vdots & \vdots & \vdots & \vdots & \vdots & \vdots & \vdots & \vdots & \ddots & \vdots & \vdots & \vdots \\ 1 & 0 & 0 & 0 & 0 & 0 & 0 & 0 & 0 & \cdots & -1 & 0 & 0 \end{array}\right). \tag{7}$$

According to equation (3), we need to update the predicted clock state using the measurements at epoch $k+1$ (i.e. $Z(k+1)$). Thus, we have

$$\begin{pmatrix} x_1(k+1) \\ f_1(k+1) \\ d_1(k+1) \\ \vdots \\ x_i(k+1) \\ f_i(k+1) \\ d_i(k+1) \\ \vdots \end{pmatrix} = \begin{pmatrix} x_1(k+1|k) \\ f_1(k+1|k) \\ d_1(k+1|k) \\ \vdots \\ x_i(k+1|k) \\ f_i(k+1|k) \\ d_i(k+1|k) \\ \vdots \end{pmatrix} + K \cdot \left(Z(k+1) - H \cdot \begin{pmatrix} x_1(k+1|k) \\ f_1(k+1|k) \\ d_1(k+1|k) \\ \vdots \\ x_i(k+1|k) \\ f_i(k+1|k) \\ d_i(k+1|k) \\ \vdots \end{pmatrix} \right), \tag{8}$$

where K is the Kalman gain matrix, which can be calculated using equation (4).

Although the above Kalman-filter time scale is quite straightforward, our clock-ensemble system is not a completely observable system because we lack an absolute time reference. Instead, we only have measurements of the time difference between each H-maser and the non-ideal reference Cs clock. Thus, we still have three degrees of freedom: the reference clock's time, frequency, and frequency drift. To limit the freedom of the reference clock's time, we require that the weighted sum of the differences between the current time estimates and their predicted values is zero, which is called the basic time-scale equation [5, 7]:

$$\sum_{i=1}^{M} w_i(k+1) \cdot x_i(k+1) = \sum_{i=1}^{M} w_i(k+1) \cdot x_i(k+1|k), \tag{9}$$

where $w_i(k+1)$ is the weight of clock i at epoch $k+1$, based on the statistics of prediction error. This constraint limits the freedom of the reference clock's time. Equation (9) has been applied to other time scales, such as the 'Kalman Plus Weights' algorithm proposed by Greenhall [4, 5] and Galleani and Tavella's time scale (see equation (58) of [8]).

However, these time scale algorithms do not limit the freedom of the reference clock's frequency and frequency drift. The freedom of the reference clock's frequency can be viewed in this way: suppose the reference clock's frequency is changing in a specific pattern, our measurement results $Z(k)$ (i.e. the time difference between each H-maser and the reference clock) are still the same as long as the other clocks' frequencies change accordingly. Thus, the reference clock's frequency can be any value, and therefore is a degree of freedom. The freedom of the reference clock's frequency drift can be viewed similarly. To limit the freedom of the reference clock's frequency and frequency drift, we need to extend the basic time-scale equation to three equations:

$$\sum_{i=1}^{M} w_{i\_x}(k+1) \cdot x_i(k+1) = \sum_{i=1}^{M} w_{i\_x}(k+1) \cdot x_i(k+1|k), \tag{10.1}$$

$$\sum_{i=1}^{M} w_{i\_f}(k+1) \cdot f_i(k+1) = \sum_{i=1}^{M} w_{i\_f}(k+1) \cdot f_i(k+1|k), \tag{10.2}$$

$$\sum_{i=1}^{M} w_{i\_d}(k+1) \cdot d_i(k+1) = \sum_{i=1}^{M} w_{i\_d}(k+1) \cdot d_i(k+1|k), \tag{10.3}$$

where there are three sets of weights, w_{i_x} for time, w_{i_f} for frequency, and w_{i_d} for frequency drift. In 2003, Senior *et al* also realized that equation (9) does not work well. Therefore, they replaced equation (9) with equation (10.2), and formed the so-called 'frequency scale' that has served as the IGS time scale for more than a decade [10]. Compared with K. Senior's time scale, the JY1 time scale uses all the three equations in equation (10) to generate the ensemble clock. w_{i_x} is determined by the uncertainty of the next-epoch time prediction error, w_{i_f} is determined by the uncertainty of the frequency after a deterministic linear fitting, and w_{i_d} is determined by the uncertainty of the frequency drift. The weights w_{i_x}, w_{i_f}, w_{i_d} are automatically updated every epoch, using an exponential filter. We need to choose proper time constants in the exponential filter, so that the weights do not change too quickly but can also be updated to reflect reality. For example, the time constant of w_{i_d} is set to 400 d. Typically, we need at least one month to estimate the frequency drift of a maser. Because w_{i_d} is determined by the statistics of the frequency drift, a time constant of a few hundred days is a reasonable value. To be more specific:

$$w_{i\_d}(k+1) \propto \frac{1}{(\sigma_{i\_d}(k+1))^2}, \text{and } (\sigma_{i\_d}(k+1))^2 = (1-\alpha) \cdot (\sigma_{i\_d}(k))^2 + \alpha \cdot (d_i(k+1) - \overline{d_i(k)})^2, \tag{11}$$

where $\sigma_{i\_d}(k+1)$ denotes the standard deviation of the frequency drift of clock i, $\overline{d_i(k)}$ denotes the average value of the frequency drift of clock i, and $\alpha = \frac{1}{400\times24\times5}$, which corresponds to the time constant of 400 d.

A simple mathematical operation can transform equations (10)–(12). Equation (12) provides a different representation of the basic time-scale equations. Here, r refers to the reference clock, which is the commercial Cs clock for our case. e refers to the ensemble (i.e. the time scale). In equation (12.1), $x_{\mathrm{er}}(k+1)$ is the estimated ensemble time with respect to the reference clock. $x_{\mathrm{ir}}(k+1)$ is the time difference between clock i and the reference clock, which is measured by the measurement system. Remember that $x_i(k+1|k)$ is the predicted time difference between clock i and the ensemble time. Thus, $[x_{ir}(k+1) - x_i(k+1|k)]$ gives the estimation of the ensemble time with respect to the reference clock, via clock i. Equation (12.1) shows that the final ensemble time is equal to the weighted sum of the ensemble-time estimation via each clock. Similarly, equations (12.2) and (12.3) show that the final ensemble frequency/frequency-drift are equal to the weighted sum of the ensemble frequency/frequency-drift estimation via each clock. From this interpretation, equation (10), which is equivalent to equation (12), not only provides the constraints to the system, but also provides the weighted method of calculating the ensemble time, frequency, and frequency drift:

$$x_{\mathrm{er}}(k+1) = \sum_{i=1}^{M} w_{i\_x}(k+1) \cdot [x_{\mathrm{ir}}(k+1) - x_i(k+1|k)], \tag{12.1}$$

$$f_{\mathrm{er}}(k+1) = \sum_{i=1}^{M} w_{i\_f}(k+1) \cdot [f_{\mathrm{ir}}(k+1) - f_i(k+1|k)], \tag{12.2}$$

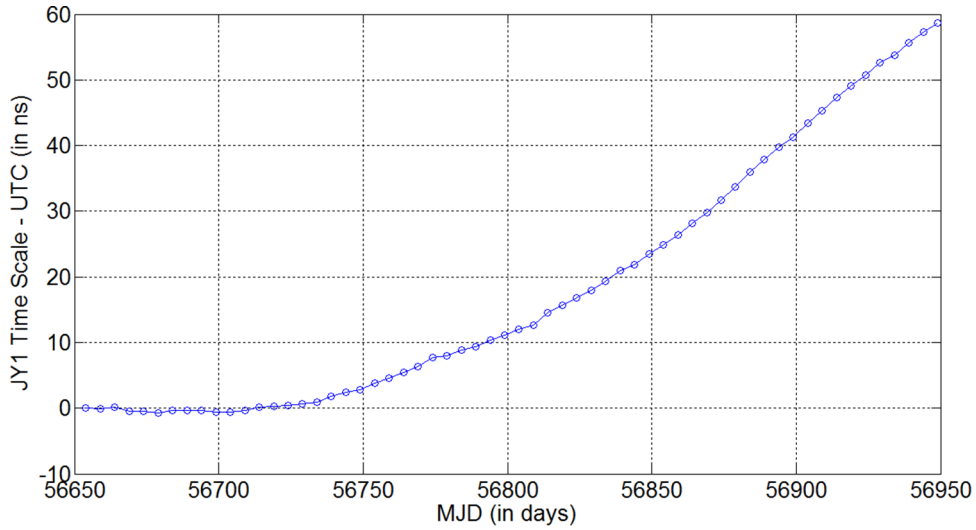

Figure 1. Free-running JY1 time scale with respect to UTC.

$$d_{\mathrm{er}}(k+1) = \sum_{i=1}^{M} w_{i\_d}\,(k+1) \cdot [d_{\mathrm{ir}}\,(k+1) - d_i(k+1|k)]. \tag{12.3}$$

Because we calculate the ensemble frequency and frequency drift based on the weights of each clock, the time scale should have better long-term stability than if we only use equation (9). As an extreme example, if a clock frequently has a large frequency drift variation or a frequency drift jump, it will pull the whole ensemble significantly if we only use equation (9). However, if we use equation (10), we can give this clock a very small weight in w_{i_d}, so that it has a small impact on the long-term stability of the time scale. We will show a real example and discuss this issue further in sections 3 and 4.

In addition to the above feature, the new Kalman-filter time scale JY1 has another new feature in comparison to the AT1 algorithm [12]. It can detect a clock time/frequency/frequency-drift error automatically. For example, for the frequency-drift error detection, if a clock's frequency drift at an epoch is more than four sigma of its frequency drift, we determine that the clock has a frequency-drift error. When the clock's frequency drift returns to less than two sigma, we add this clock back to the ensemble and give this clock its normal weights. This algorithm is good for detecting short-term outliers in the frequency drift. Some H-masers have a small long-term linear change in the frequency drift, and the above algorithm does not work well for such a clock error. To detect this type of frequency-drift error, we do a linear fit of the frequency drift over tens of days. If the ratio of the slope to the uncertainty of the slope is greater than 5, then we determine that this clock does have a long-term change in frequency drift and remove it from the ensemble. As for the frequency error detection, we do a similar four-sigma error detection. Thanks to the 12 min interval for the estimation of time, frequency, and frequency drift, we can find a clock error quickly and remove the bad clock from the ensemble before it pulls the ensemble too much.

These two novel features make the new time scale stiff and less likely to be affected by a bad clock. We will test the performance of this time scale in the next section.

3. Performance of free-running time scale

We ran the JY1 time scale for Modified Julian Date (MJD) 56 650.0–56 950.0. For test purposes, we only used four H-masers in the time scale, so that it was less complicated. At 56 650.0, we initialized the time scale, by estimating the clock states (time, frequency, and frequency drift) with respect to UTC (Coordinated Universal Time). In this way, the time scale was well aligned with UTC at the very beginning. Then we let the time scale completely free-run. The result is shown in figure 1. We can see that after 100 d of free running (i.e. at 56 750.0), the time scale is only ~3 ns away from UTC. This illustrates that the new time scale is quite stiff. Because the time scale is composed of H-masers and an H-maser can exhibit some small change in frequency drift, the time scale typically has a non-zero frequency drift in the very long term (>100 d), as indicated in figure 1. The frequency drift is approximately 2.5×10^{-22} s s^{-2}, in this case.

Figure 2 shows the frequency drift of the H-masers with respect to the time scale. Overall, all four H-masers have quite stable frequency drift. The mean values of the frequency drifts are -3.5×10^{-22} s s^{-2}, -34.8×10^{-22} s s^{-2}, -167.8×10^{-22} s s^{-2}, and -7.4×10^{-22} s s^{-2}, for ST0005, ST0006, ST0007, and ST0022, respectively. However, we can still see some abnormal behavior in the frequency drift from time to time. For example, there is a spike in ST0005 around MJD 56 868.7. Checking the ST0005 environmental chamber temperature data, we found a temperature spike around MJD 56 868.6. This confirms that our estimation of frequency drift is done properly and can reflect the actual physical change of a clock. For another example, there is a change in the red curve of figure 2 (ST0005), starting from around MJD 56 915. By checking the chamber temperature for ST0005, we found that this clock change corresponds to a temperature change from

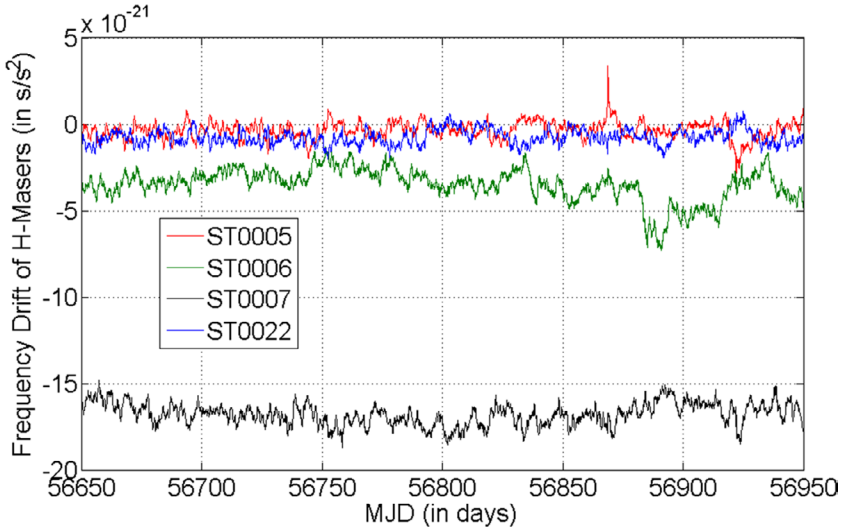

Figure 2. Frequency drift of H-masers.

25.3 °C to 25.2 °C at around 56 914. We should mention that the change in the chamber temperature is small (only 0.1 °C) and there is some delay for the whole H-maser to change to 25.2 °C. Also, the Kalman filter, as a low-pass filter, causes some delay in the updates of a clock's state. Thus, we have a 1 d latency in clock error detection in this case.

As we have mentioned in section 2, once a clock error is detected, we give the clock 0 weights in the three equations of equation (10), no matter what the physical reason is. In this way, the time scale is not affected by an abnormal clock. If the clock error disappears later, it regains its normal weights.

From figure 2, it is clear that an H-maser is not always well behaved. If we steer a single H-maser to the Cs fountain, it is quite likely to have a large timing error when the fountain stops working. In contrast, if we have an ensemble of H-masers, we can detect a bad clock and mitigate its impact. In this way, we may have still a small timing error, but we can avoid a large timing error.

Next, we simulate a frequency jump and a frequency-drift jump in a clock, and see how much the output of the JY1 time scale changes due to these jumps. Ideally, we want to detect the frequency/frequency-drift errors and remove the clock from the ensemble immediately when the errors occur. Practically speaking, the filtering process, as a kind of a low-pass filter, will lead to some time delay in reflecting the actual jump in frequency or frequency drift (because a jump contains all frequencies in the frequency domain). Also, we determine if there is a frequency/frequency-drift error based on the criteria that the frequency/frequency-drift at the current epoch is greater than four times the standard deviation of the frequency or frequency drift. Thus, it is difficult to completely eliminate the impact of the frequency/frequency-drift error of a clock. Nevertheless, by giving the clock 0 weights in equation (10), once we determine that the clock is bad, we can still mitigate the impact significantly.

Figure 3 shows an example. We artificially add a frequency jump of 6.8×10^{-15} s s^{-1} in ST0006 at MJD 56 700.0. This frequency jump corresponds to around a 2 °C H-maser chamber temperature change [13]. Because of this frequency jump, ST0006 would be 147 ns away from what ST0006 should be, at MJD 56 950.0. Thanks to the advanced error-detection algorithm and the three basic time-scale equations (i.e. equation (10)), the JY1 time scale is pulled by only ~3.5 ns at MJD 56 950.0 (see the red curve in figure 3). Similarly, we artificially add a frequency-drift jump of 5.36×10^{-21} s s^{-2} in ST0006 at MJD 56 700.0. Because of this frequency-drift jump, ST0006 would be 1250 ns away from what ST0006 should be, at MJD 56 950.0. We want to address that this jump value is very big and rarely happens in practice. The blue curve in figure 3 shows the performance of the JY1 time scale in such an extreme situation. We can see that the JY1 time scale is pulled by only ~23.6 ns at MJD 56 950.0.

From the above analysis, the new time scale JY1 is stiff and relatively immune to abnormal clock behaviors, especially when the clock error is not large.

4. Steering the time scale to a Cs fountain

In section 3, we have demonstrated that the new time scale JY1 is stiff and cannot easily be pulled by a bad clock. Thus, it can serve as a good flywheel. If it is steered to a Cs fountain, the final output can be accurate, precise, and reliable.

At NIST, we have run the NIST F1 Cs fountain [14] during MJD 57 264.9–57 287.8, 57 360.0–57 374.0, and 57 420.8–57 439.0. The fountain-operation periods are labeled by red rectangles in figure 4. Here, we run the time scale during MJD 56 980.0–57 500.0, and steer it to the Cs fountain. Note, the steering algorithm corrects both the frequency and the frequency drift of the free-running time scale, using the Cs fountain.

The free-running time scale is composed of six H-masers and a reference commercial Cs clock. The H-masers are ST0005, ST0006, ST0007, ST0010, ST0012, and ST0022. At MJD 56 980.0, the time scale is aligned with the UTC. The blue curve in figure 4 shows the result of the free-running time scale. We can see that the free-running time scale has a very good match ($<\pm 1$ ns) with UTC during MJD 56 980.0–57 080.0. This again confirms that the time

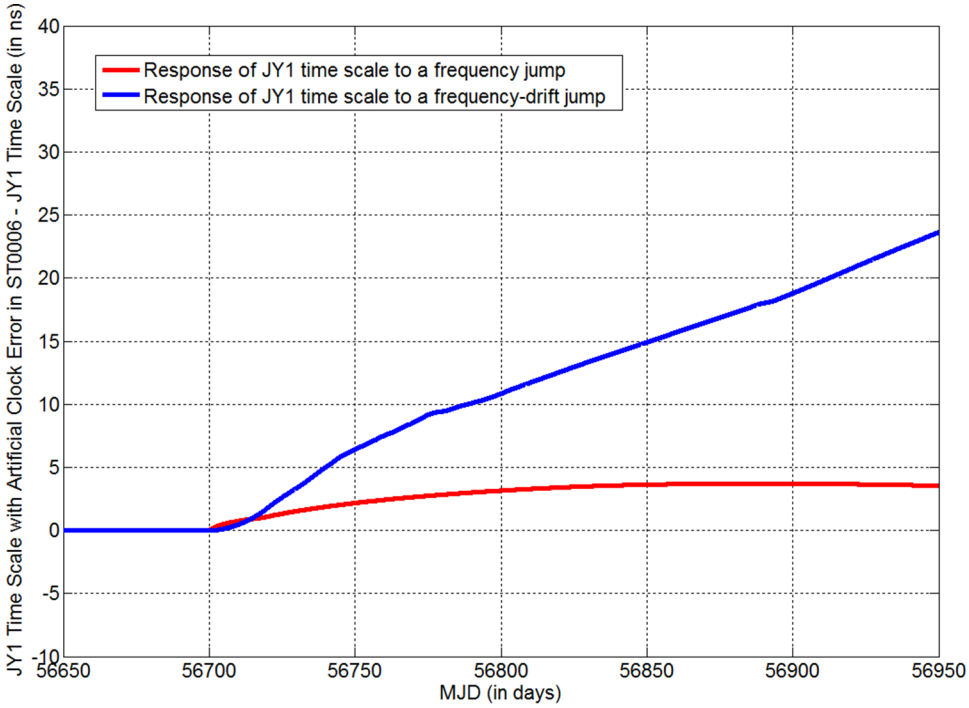

Figure 3. Response of the JY1 time scale to a frequency jump (red curve) or a frequency-drift jump (blue curve). For the red curve, we artificially add a frequency jump of 6.8×10^{-15} s s^{-1} in ST0006 at MJD 56 700.0. For the blue curve, we artificially add a frequency-drift jump of 5.36×10^{-21} s s^{-2} in ST0006 at MJD 56 700.0.

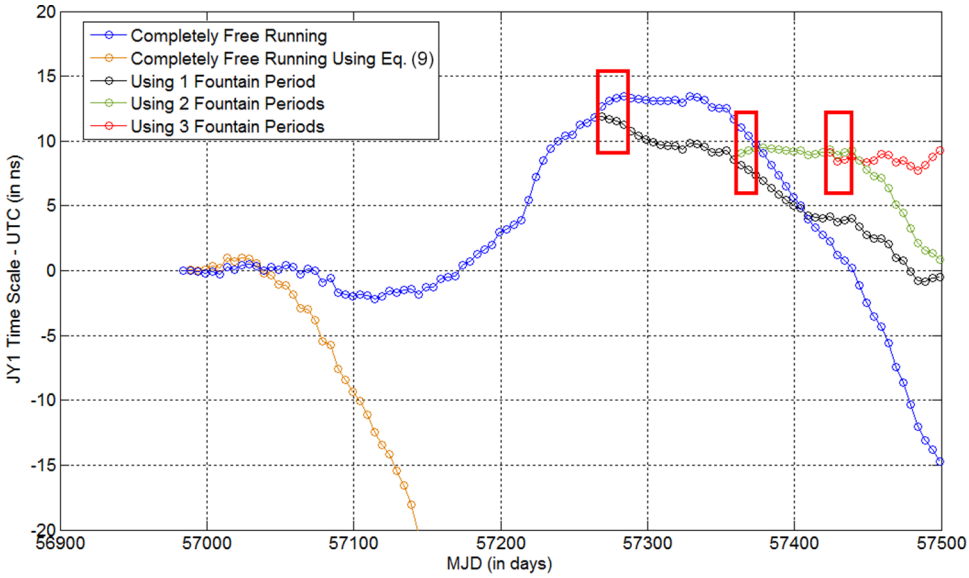

Figure 4. Steering the free-running JY1 time scale to the NIST F1 Cs fountain. We compare the time scale with the UTC. Note, the black, green, and red curves are the same as the blue curve during MJD 56 980.0–57 264.9; the green and red curves are the same as the black curve during MJD 57 264.9–57 360.0; the red curve is the same as the green curve during MJD 57 360.0–57 420.8. The blue curve shows the completely free running using equation (10), while the orange curve shows the completely free running using equation (9). The clock-error detection function described in section 2 has already been used in the blue curve and the orange curve.

scale is good at keeping time for approximately three months once it is initially aligned with the UTC or a Cs fountain. After MJD 57 080.0, the time scale starts to have a small positive frequency drift. Because of this frequency drift, the time scale starts to depart from UTC, and at ~MJD 57 230 it is ~10 ns away from UTC. Then its frequency drift slowly becomes negative, and at MJD 57 500 it is ~ −15 ns away from UTC. As a comparison, the orange curve shows the free-running time scale using equation (9), instead of using equation (10). Clearly, the time scale using equation (9) diverges from UTC after about 20–30 d. At MJD 57 500.0, it is about −270 ns away from UTC. Thus, it is not as stiff as the JY1 time scale.

Next, we steer the JY1 time scale to the first Cs fountain period (i.e. MJD 57 264.9–57 287.8). The result is shown by the black curve. By comparing the black curve with the blue

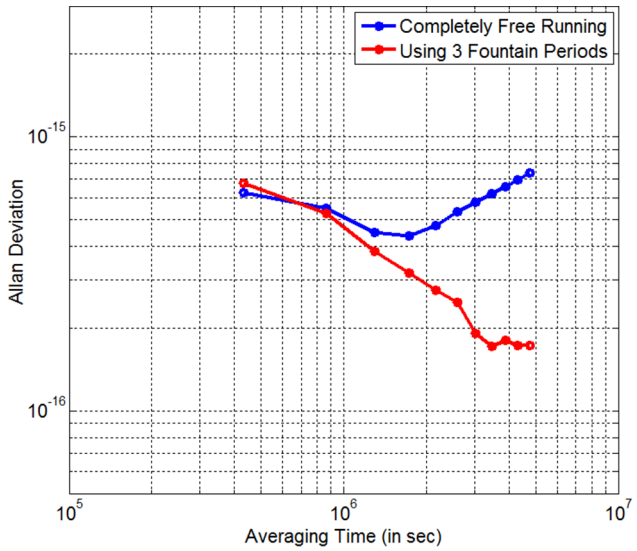

Figure 5. The frequency stability of the time scale using three fountain periods (red curve), versus the frequency stability of the free-running time scale (blue curve), for MJD 57 264.0–57 500.0.

curve during MJD 57 264.9–57 500.0, we find that because of using the Cs fountain, the frequency drift in the free-running time scale is removed. Also, the large frequency offset at 57 264.9 in the blue curve is corrected by the Cs fountain. The black curve departs from the UTC by less than ~5 ns for the first 90 d (i.e. 57 287.8–57 377.8) after the time scale is steered to the fountain.

The green curve is the result of steering the free-running time scale to the two Cs fountain periods (i.e. MJD 57 264.9–57 287.8, and MJD 57 360.0–57 374.0). Note, the green curve is the same as the black curve during MJD 57 264.9–57 360.0. Again, the green curve drifts from the UTC by less than ~5 ns for the first 90 d (i.e. 57 374.0–57 464.0) after the time scale is steered to the fountain.

Lastly, the red curve shows the result of steering the free-running time scale to the three Cs fountain periods (i.e. MJD 57 264.9–57 287.8, 57 360.0–57 374.0, and 57 420.8–57 439.0). During 57 264.9–57 500.0, the red curve has a change of less than 4 ns with respect to the UTC. Figure 5 shows a frequency-stability analysis of the free-running time scale and the time scale using three fountain periods, during 57 264.0–57 500.0. Figures 4 and 5 show that the improvement from steering to the Cs fountain is significant in both time and frequency stability. Note that the Cs fountain was operated for only 55 d over the whole 235 d duration of the test. In other words, with the Cs fountain running for less than 25% of the time, we successfully maintain the time within 4 ns. This opens a new possibility for designing a time scale. To achieve less than 5 ns of error, we only require the Cs fountain to be operated occasionally, instead of having a continuously-operated Cs fountain. This can be helpful when we do not have a continuously operated fountain. Also, a continuously operated fountain may accidentally stop. By using our new time scale algorithm, we allow ~3 months for repairs. During the three months, the timing error is at most 5 ns, according to the tests shown here. Most importantly, nowadays NIST has many excellent optical clocks under active development. However, it is difficult to run optical clocks for a long time (>a few days), due to engineering obstacles. Because of this, it is believed that an optical clock cannot contribute to the time scale for the time being. However, from this example we can imagine that occasional optical-clock operation (e.g. 4 h every week) could be very helpful for the long-term (e.g. >20 d) performance of the time scale. Thus, instead of waiting until all engineering obstacles are solved, we should consider incorporating an optical clock into the time scale now.

5. Summary

This paper discusses a new Kalman-filter hydrogen-maser time scale JY1 developed at NIST. The JY1 time scale is designed to be stiff and nearly immune to abnormal clock behavior. Tests show that when the time scale is initially aligned to UTC and then is free running, it deviates from the UTC by less than ±5 ns for ~100 d. Thus, it is a good flywheel. Once the time scale is steered to a Cs fountain, it can maintain the time with little error (<4 ns) even if the Cs fountain stops working for tens of days. Thus, an occasionally operated Cs fountain is good enough to significantly improve the accuracy of the time scale. This time scale algorithm also makes incorporating an occasionally operated optical clock into the clock ensemble possible.

Acknowledgments

The authors thank Stefania Romisch, Josh Savory, Jeff Sherman, Trudi Peppler, Steve Jefferts, and Tom Heavner for maintaining the NIST time scale and the NIST F1 fountain. The authors also thank Neil Ashby, Jeff Sherman, and Mike Lombardi for their comments.

References

[1] Breakiron L A 1991 Timescale algorithms combining Cesium clocks and Hydrogen masers *Proc. 23rd Annual Precise Time and Time Interval (PTTI) Systems and Applications Meeting* pp 297–302
[2] Rovera G D, Bize S, Chupin B, Guena J, Laurent P, Rosenbusch P, Uhrich P and Abgrall M 2016 UTC(OP) based on LNE-SYRTE atomic fountain primary frequency standards *Metrologia* **53** S81–8
[3] Bauch A, Weyers S, Piester D, Staliuniene E and Yang W 2012 Generation of UTC(PTB) as a fountain-clock based time scale *Metrologia* **49** 180–8
[4] Greenhall C A 2001 Kalman plus weights: a time scale algorithm *Proc. 33rd PTTI Meeting* pp 445–54
[5] Greenhall C A 2012 A review of reduced Kalman filters for clock ensembles *IEEE Trans. UFFC* **59** 491–6
[6] Greenhall C A 2003 Forming stable timescales from the Jones–Tryon Kalman filter *Metrologia* **40** S335–41
[7] Galleani L and Tavella P 2003 On the use of the Kalman filter in timescales *Metrologia* **40** S326–34
[8] Galleani L and Tavella P 2010 Time and the Kalman filter *IEEE Control Syst. Mag.* **30** 44–65

[9] Stein S R 1992 Advances in time-scale algorithms *Proc. 24th PTTI Meeting* pp 289–302
[10] Senior K and Koppang P 2003 Developing an IGS time scale *IEEE Trans. UFFC* **50** 585–93
[11] Gelb A 1974 *Applied Optimal Estimation* (Cambridge, MA: MIT Press)
[12] Levine J 2012 The statistical modeling of atomic clocks and the design of time scales *Rev. Sci. Instrum.* **83** 021101
[13] Parker T 1999 Environmental factors and hydrogen maser frequency stability *IEEE Trans. UFFC* **46** 745–51
[14] Jefferts S R *et al* 2002 Accuracy evaluation of NIST-F1 *Metrologia* **39** 321–36